JACS
JOURNAL OF THE AMERICAN CHEMICAL SOCIETY

Article

pubs.acs.org/JACS

Stacking Interactions Induced Selective Conformation of Discrete Aromatic Arrays and Borromean Rings

Long Zhang, Lin Lin, Dong Liu, Yue-Jian Lin, Zhen-Hua Li, and Guo-Xin Jin*

Shanghai Key Laboratory of Molecular Catalysis and Innovative Materials, State Key Laboratory of Molecular Engineering of Polymers, Collaborative Innovation Center of Chemistry for Energy Materials, Department of Chemistry, Fudan University, Shanghai 200433, P. R. China

Supporting Information

ABSTRACT: Herein, we describe how to utilize stacking interactions to achieve selective supramolecular transformation and molecular Borromean rings (BRs). By using a dinuclear naphthalenediimide (NDI)-based Cp*Rh acceptor and linear bipyridyl ligands, organometallic rectangles featuring dynamic behavior have been constructed. Unique discrete aromatic stacking arrays were formed by inducing pyrene units as guest molecules. The topology of the BRs was realized by the use of a strategically chosen ligand which was capable of participating in D−A interactions and hydrogen bonding, as evidenced from single-crystal X-ray analysis and computational studies. These self-assembly processes underline the advantages of dynamic bonding and $\pi-\pi$ stacking interactions, and serve to illustrate a new approach to generating structurally and topologically nontrivial supramolecular architectures.

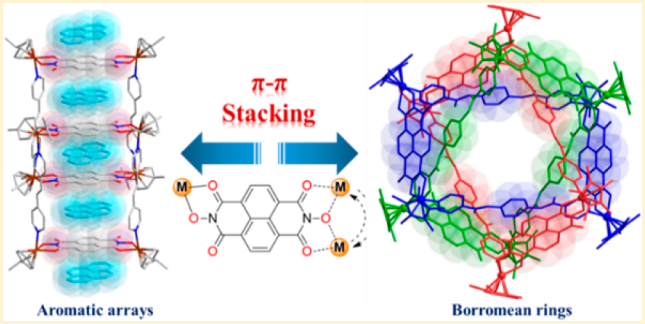

INTRODUCTION

In recent years, a large amount of supramolecular coordination complexes have been constructed using well-established design principles.[1−4] In order to reduce the generation of isomers, the building blocks are usually designed to be rather rigid and highly symmetric.[5] As a result, the prepared artificial assemblies tend to also be rigid. In contrast, functional structures in biological systems, such as proteins, are inherently dynamic and sample a vast ensemble of conformations.[6] Thus, the exploration of architectures that have the ability to adjust their shape and conformation is very interesting.[7]

In chemical and biological processes, noncovalent interactions are of crucial relevance. These interactions play a pivotal role in supramolecular chemistry,[8] such as DNA/RNA stacking, drug recognition, protein folding, and crystal engineering.[9] Among these, the electrostatic interactions between electron-rich (donor, D) and electron-deficient (acceptor, A) aromatics are important driving forces, which have been used in the self-assembly of structurally and topologically nontrivial structures, such as stacked aromatics, molecular knots, and links.[10] However, the relationship between the chemical structures of building blocks and the resulting assemblies is not well-established, and it is still a significant challenge to synthesize more complex topologies such as molecular Borromean rings (BRs),[11] David catenanes,[12] trefoil knots,[13] and Solomon links.[14] In order to elucidate the rational design principles of such intriguing architectures, new reports of this type will be crucial, and may inspire the construction of simple molecular machines.[15]

Here, we reported the preparation of a new class of metallarectangles featuring dynamic conformations. The naphthalenediimide (NDI)-based ligand L_1 was chosen because of its dynamic coordination modes (Scheme 1), which can allow the assembly to "error check" to seek the thermodynamic minimum.[16] More importantly, its planar, electron-deficient aromatic surface can engender favorable aromatic D−A π interactions.[17] Conformation selection was achieved by guest-induced transformation processes. Discrete quintet and nonet aromatic stacking structures were formed by utilizing favorable pyrene-NDI π-stacking interactions. Furthermore, we also show that D−A stacking interactions can enable the template-free self-assembly of a BRs structure, and density functional theory (DFT) calculations were used to provide insight into the formation of molecular BRs.

Scheme 1. Coordination Mode of L_1

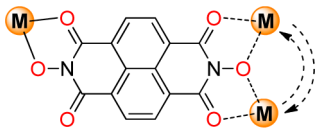

Received: November 19, 2016
Published: January 9, 2017

DOI: 10.1021/jacs.6b11968
J. Am. Chem. Soc. 2017, 139, 1653−1660

RESULTS AND DISCUSSION

The reaction of $[Cp^*RhCl_2]_2$ (2.0 equiv) with DHNDI (1.0 equiv) in the presence of AgOTf (4.0 equiv) and NaOH (2.0 equiv) produced dirhodium complex **1**, which has two types of structures: the *cis* form and the *trans* form (Scheme 2). The

Scheme 2. Synthesis of Dinuclear Complex 1

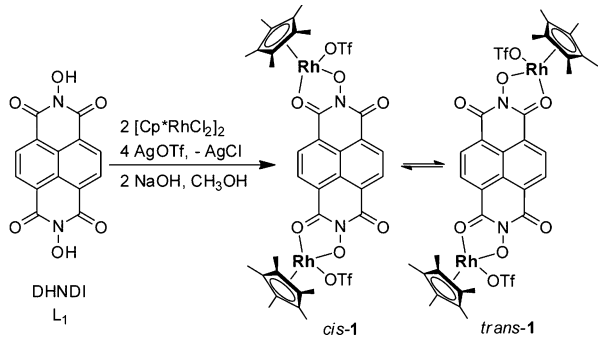

structure of **1** was confirmed by electrospray ionization mass spectrometry (ESI-MS) and ^{1}H NMR spectroscopy. The ESI-MS data of **1** in CH_3OH shows a peak at 921.0 m/z assigned to $[\mathbf{1} - OTf]^+$, which indicates that complex **1** is stable in solution. The variable-temperature ^{1}H NMR spectrum of **1** in CD_3OD indicated the dynamic exchange of **1** between *cis* and *trans* conformations in solution. At room temperature (298 K), the NDI group showed only one singlet at δ 8.81, while at a lower temperature (213 K), the signals were broadened and split, suggesting that the two conformations of **1** convert slowly on the ^{1}H NMR time scale.

The solid-state structure of **1** was elucidated by single-crystal X-ray analysis. The crystal structure revealed a *cis* conformation composed of two half-sandwich Cp*Rh groups bridged by the NDI ligand (Figure 1a). The distance between two Rh metal

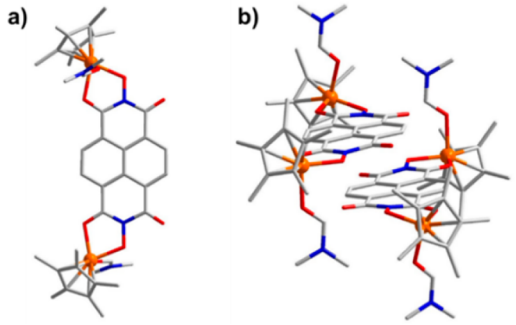

Figure 1. (a) Molecular structure of the cation of **1**, with each rhodium center bearing one DMF molecule and (b) its stacking mode. Counteranions and hydrogen atoms are omitted for clarity (N, blue; O, red; C, gray; F, green; S, yellow; Rh, orange).

centers is about 11.2 Å. The two Rh centers are coordinated by two DMF molecules, forming a three-legged piano stool geometry. In contrast to the *trans* conformation, the *cis* conformation is beneficial for the $\pi-\pi$ stacking interactions between two NDI backbones, with a distance of 3.3 Å (Figure 1b).

Self-Assembly of Metallarectangles. To construct the metallarectangles, dinuclear complex **1** was treated with rigid linear pyridyl ligands (L_n) in a 1:1 molar ratio (Scheme 3). As a result of random combinations of two conformations of **1** and

Scheme 3. Self-Assembly of Complexes 2−6

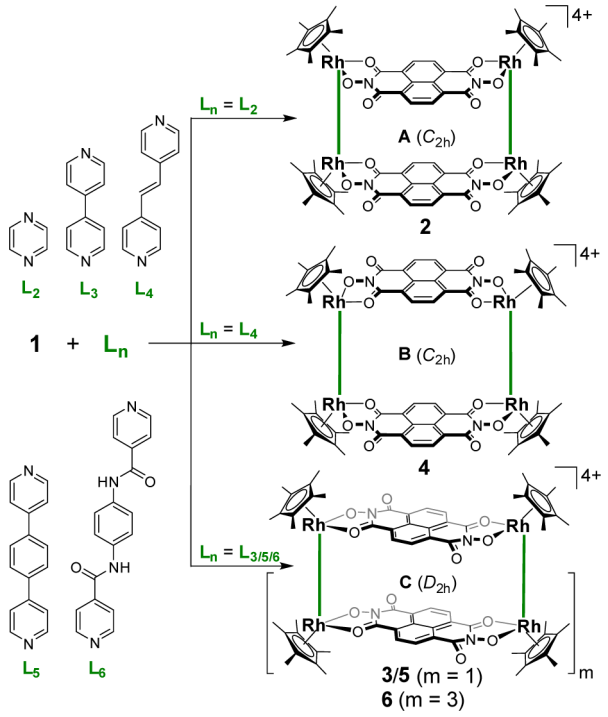

different orientations of the NDI groups, there would be different isomers that may be formed upon the self-assembly of metallarectangles in the absence of any biasing interactions. From the perspective of thermodynamics, the favorable product is the structure with the lowest binding free energy. Therefore, three symmetrical configurations (**A**/**B**/**C**) are selected (Scheme 3), which are confirmed by X-ray crystallographic analysis.

In solution, due to the dynamic nature of the dinuclear metal clips, the configuration of the metallarectangles can transform between the three isomers, as evidenced by broad peaks for the NDI group in ^{1}H NMR spectra (see Supporting Information).

The solid-state structures of complexes **2**−**5** were determined by single-crystal X-ray diffraction analysis, and were confirmed to be monomeric rings. Interestingly, the length of the pyridyl arm influences the configuration of these metallarectangles in the solid state. The crystal structure of **2** revealed the complex cation to have topology **A**, which adopts an approximate C_{2h} point symmetry, with dimensions of 11.2 and 7.0 Å (Rh···Rh nonbonding distances, Figure 2). The two NDI groups of dinuclear acceptor units are oriented in the same

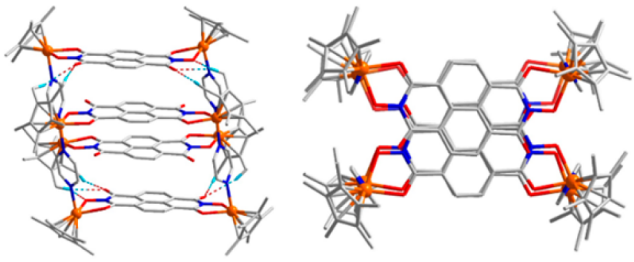

Figure 2. Single-crystal X-ray structure of **2**: side view (left) and top view (right). Counteranions and hydrogen atoms are omitted for clarity except for those involved in hydrogen bonding. (N, blue; O, red; C, gray; Rh, orange; H, light blue).

DOI: 10.1021/jacs.6b11968
J. Am. Chem. Soc. 2017, 139, 1653−1660

direction. As shown in Figure 2, two identical rectangles of **2** were partially stacked without interlocking, which is stabilized by parallel $\pi-\pi$ stacking in the range 3.24–3.36 Å. Moreover, hydrogen bonds were formed between the O atoms of the outside NDI units and the Cp* protons, with distances ranging from 2.27 to 2.76 Å. The D_{2h} isomer **C** was observed when using longer linkers L_3 and L_5. According to the crystal structures of **3** and **5** (Figure 3a,c), the distance between two

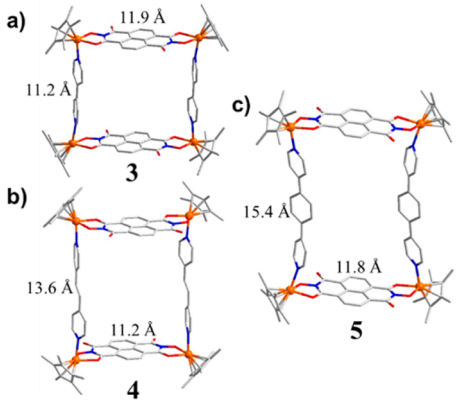

Figure 3. Single-crystal X-ray structure of **3** (a), **4** (b), and **5** (c). Counteranions and hydrogen atoms are omitted for clarity (N, blue; O, red; C, gray; Rh, orange).

Rh centers of the *trans* form of the dinuclear acceptor is about 11.9 Å, which is longer than that of the *cis* form. The **B** configuration was achieved by using L_4 (*trans*-1,2-bis(4-pyridyl)ethene) as the bridging ligand, with dimensions of 11.2 × 13.6 $Å^2$ (Rh–Rh nonbonding distances, Figure 3b).

Self-Assembly of Aromatic Arrays. To investigate the guest-induced rearrangements upon the formation of the metallarectangles, the π-electron-rich molecule pyrene, with a similar backbone to the NDI units, was selected as guest molecule (Scheme 4). A methanol solution of **3** was stirred with excess pyrene (6.0 equiv) at room temperature. The resulting product **3a** was washed with ether to remove the excess pyrene. In the ^{1}H NMR spectrum of **3a**, the pyrene protons were observed as three broad signals at 7.01, 6.75, and 6.00 ppm. The large upfield shift of the pyrene protons is presumably due to the strong shielding effect of the NDI moieties. According to the integral ratios of pyrene protons and Cp* protons, the stoichiometry of complex **3** and pyrene is 2:1, indicating that two metallarectangles share one pyrene guest molecule. The structure of **3** in solution was also supported by ESI-MS. The prominent peaks at m/z = 1128.19 ($[\mathbf{3a} - 4OTf^- - 4H]^{4+}$) and 1554.17 ($[\mathbf{3a} - 3OTf^- - 2H]^{3+}$) were in good agreement with their theoretical distribution (Figure S45), suggesting that this formation is intact in solution. The solid-state structure was unambiguously confirmed by X-ray crystallographic analysis.

Single crystals suitable for X-ray structure determination were obtained by slow vapor diffusion of diethyl ether into a methanol solution of **3a**. In the resulting structure, the conformation of **3** was found to change to topology **A**. As shown in Figure 4, a pyrene molecule was found to be encapsulated in the void of two partially stacked metallarectangles, providing a well-defined quintet stacking structure. As a result, the five aromatic molecules are efficiently layered with maximum overlap, stabilized by parallel-displaced $\pi-\pi$

Scheme 4. Self-Assembly of Aromatic Arrays 3a and 4a

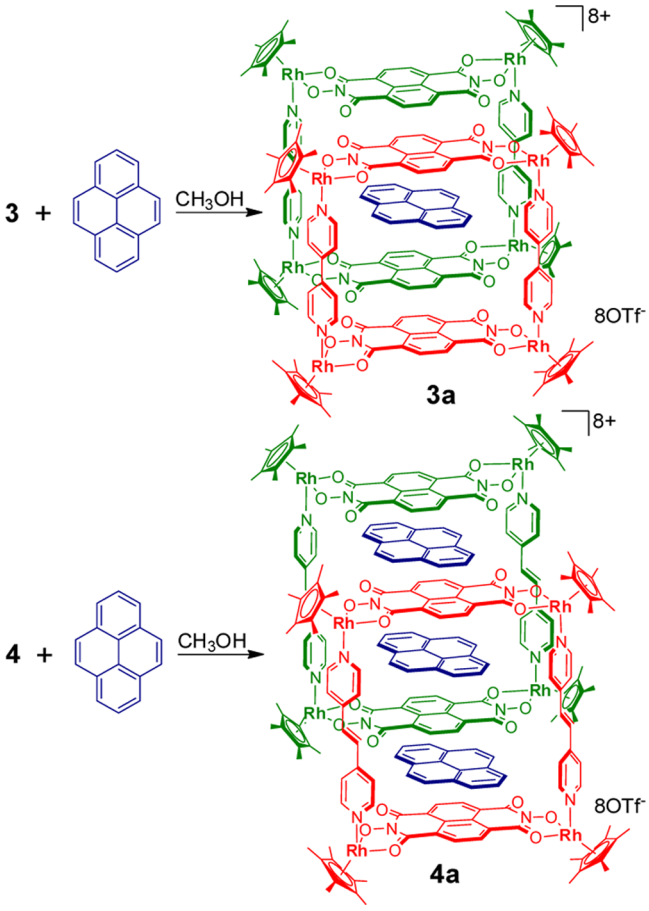

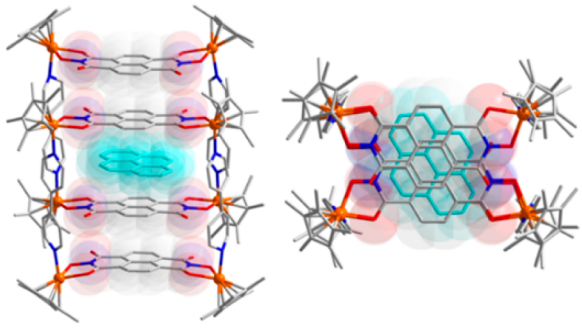

Figure 4. Single-crystal X-ray structure of **3a**: front view (left) and top view (right). Counteranions are omitted for clarity.

stacking (3.5 Å) and edge-to-face-type CH–π interactions (2.7 Å) between pyrene and pyridyl rings. Similar to the stacked mode of complex **2**, hydrogen bonds were also observed between the O atoms of the outside NDI units and the Cp* protons in the range 2.26–2.66 Å.

The reaction of rectangle **4** with pyrene in methanol produced a black crystalline precipitate of **4a**. The structure of **4a** was clearly revealed in solution by detailed NMR studies (see Supporting Information). Although initial attempts to obtain single crystals suitable for X-ray analysis were fruitless, probably due to the fast assembly being detrimental for crystal packing, the structure of complex **4a** was unambiguously confirmed by the X-ray crystallographic analysis of the analogous complex **4a′** (where the Cp*Rh fragments are replaced by (*p*-cymene)Ru). Single crystals suitable for X-ray

DOI: 10.1021/jacs.6b11968
J. Am. Chem. Soc. 2017, 139, 1653–1660

analysis were grown by a heterogeneous layer diffusion method, where a CH_3OH solution of **4′**[18] was placed at the bottom of a culture tube, followed by careful layering of a hexane solution of pyrene (excess). The crystallographic analysis confirmed that the structure of **4a′** (Figure 5) was similar to that of **3a**. The

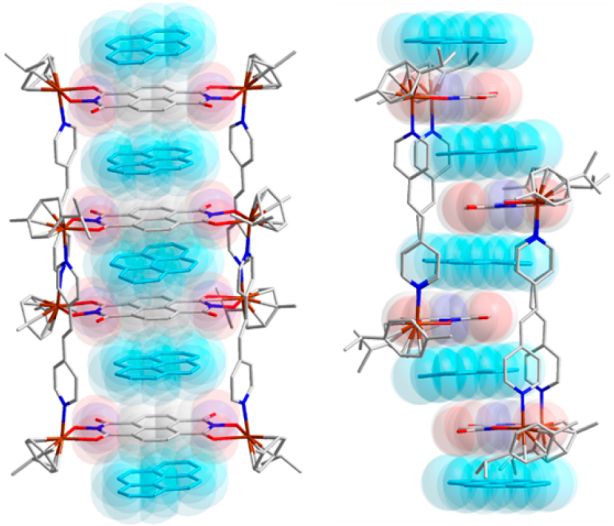

Figure 5. Single-crystal X-ray structure of **4a′**: front view (left) and side view (right). Counteranions are omitted for clarity.

topology of **4′** had also changed to **A**-type. Two metallarectangles of **4′** were connected by three guest pyrene molecules via $\pi-\pi$ stacking interactions between the guests and the NDI units. Another two pyrene molecules were found to be stacked outside the assembly. However, no infinite columnar structure was formed; instead, a unique nonet aromatic stacking structure was observed (Figure 5), which is similar to the aromatic stacking structures reported by Fujita et al.,[10b] but with no interpenetration between the two rectangles. The height of this aromatic column is about 2.6 nm, corresponding to an octuple $\pi-\pi$ stacking distance (3.3 Å). As the NDI and pyrene units are electron-deficient (acceptor, A) and electron-rich (donor, D), respectively, **2** and **3a** can be seen as A−A−A−A and A−A−D−A−A arrays, respectively, whereas **4a′** is a D−A−D−A−D−A−D−A−D stack.

The larger rectangle **5** was also treated with potential guest molecule pyrene; however, no change was observed in the ^{1}H NMR spectrum of the reaction mixture, probably due to the inappropriate Rh−Rh distance (15.4 Å).[2] Moreover, as the bridging ligand becomes longer, the cavity of the rectangle becomes too large to form a stable stack structure without interpenetration.

Self-Assembly of Borromean Rings. The binding of electron-rich pyrene within rectangles **3** and **4** prompted us to explore the synthesis of molecular BRs by employing a bridging ligand with a suitable electron-rich central group. We speculated that favorable D−A stacking interactions between dinuclear building block **1** and a suitable bridging ligand may enable the self-assembly of BRs assemblies. On the basis of our previous studies,[19] in which the design principles of BRs were established, we carefully selected bridging ligands of suitable length. The length of the short-arm linker (*trans*-**1**) is ca. 11.9 Å, which is large enough to allow the bridging ligand with a phenyl group to pass through. The ideal NDI−NDI parallel distance (long arm length) is ca. 11.9 + 3.5 Å ($\pi-\pi$ stacking distance) × 2 = ca. 18.9 Å, which corresponds to the length of bridging ligand plus double the Rh−N distance (2.1 Å × 2). Thus, the length of the pyridyl arm should be 14.7 Å. Diamide pyridyl ligand L_6 was chosen for this purpose (Scheme 3), which could be prepared easily. Although the length of L_6 is ca. 15.6 Å, the relative flexibility of L_6 would satisfy the requirements. Moreover, the potential hydrogen bonding between carbonyl oxygen atoms and amide protons can also possibly be attributed to the templating effects.[20]

As expected, the resulting BRs structure **6** was formed, as revealed by NMR studies. The ^{1}H NMR spectrum of **6** is much more complex than that of the other metallarectangles, indicating a more complex topological structure. Most of the proton resonances were found to be split into two signals rather than the simple resonances previously observed. Especially, two sets of doublets for the phenylene protons were observed at 5.75 and 5.34 ppm. The significant upfield shift of the phenylene proton resonances is due to the increased shielding by the π-acceptor NDI moieties of the outer rectangle. The ^{1}H diffusion-ordered spectroscopy (DOSY) NMR spectrum of **6** (Figure S33) showed that the aromatic and Cp* signals displayed a single diffusion constant, suggesting that only one stoichiometry of assembly was formed. The ESI-MS data also indicated that complex **6** in solution would preserve its trimeric structure: $[\mathbf{6} - 5OTf^- - 7H]^{5+}$ (m/z = 1517.34) and $[\mathbf{6} - 4OTf^- - 6H]^{4+}$ (m/z = 1933.72) (Figure S48). It should be noted that BRs **6** can convert into monomeric rings. In a dilute CD_3OD solution (0.5 mM), the formation of monomeric rectangle **6** was observed in small amounts, as new peaks were observed at 8.84 (d), 7.98 (d), 7.59 (s), and 1.78 (s) ppm in the ^{1}H NMR spectrum (Figure S34). Moreover, solvent-induced supramolecular transformation was also observed. In the DMF solution of **6**, only monomeric rectangle **6** was formed, as monitored by NMR studies (see Supporting Information). This is presumably because the interaction of $\pi-\pi$ stacking and hydrogen bonds has been weakened by DMF molecules. Similar phenomena have been observed in a recent study on BRs structures.[11d] Although monomeric rectangles of **6** can exist in a dilute solution, only black crystals of BRs **6** were obtained in quantitative yield upon vapor diffusion of diethyl ether into the CH_3OH/DMF solution of **6**.

The X-ray structure of **6** unambiguously confirmed the BRs structure (Figure 6c,d), wherein three interpenetrating but noncatenated rectangles make up an inseparable ensemble. Each of the three equivalent rings adopted a topology **C** configuration with dimensions of 11.8 and 19.7 Å (Rh−Rh nonbonding distances) (Figure 6a,b). As expected, **6(BRs)** is stabilized by strong $\pi-\pi$ (3.5 Å) stacking interactions between phenyl moieties of L_6 and NDI moieties of **1**, and six amide hydrogen bonds between O atoms of the inner rectangle and N−H moieties of the outer rectangle, with distances ranging from 2.10 to 2.21 Å. In addition, the analogous Cp*Ir-based BRs complex **6′** can also be constructed (Figure S1). In order to gain insight into the formation of **6(BRs)**, DFT binding energy calculations were performed to study the intermolecular interactions in **6(BRs)** (Table S9). The formation energy of the Borromean structure from three monomers of **6** was evaluated to be −114.7 kcal/mol. The contribution energies of $\pi-\pi$ stacking and hydrogen bonding were found to be −61.7 and −53.0 kcal/mol, respectively.

DOI: 10.1021/jacs.6b11968
J. Am. Chem. Soc. 2017, 139, 1653−1660

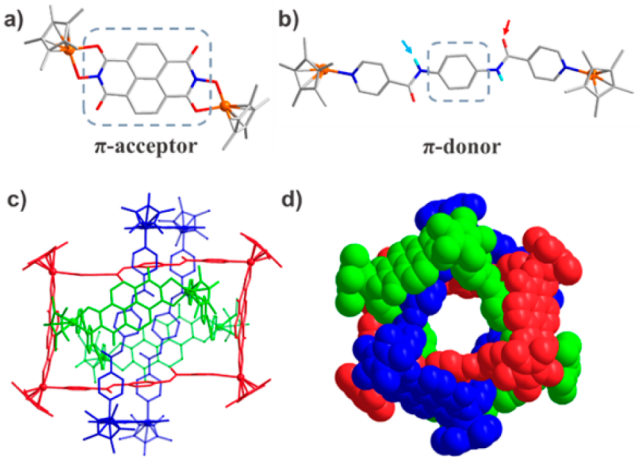

Figure 6. X-ray structure of **6(BRs)**. (a, b) Short arm and long arm (N, blue; O, red; C, gray; Rh, orange; H, light blue), hydrogen bond donor (turquoise arrow), and hydrogen bond acceptor (red arrow). (c, d) Ball-and-stick and space-filling presentations. Counteranions are omitted for clarity.

CONCLUSIONS

In conclusion, we present here a class of dynamic conformational assemblies constructed through stepwise coordination-driven self-assembly, by using a Cp*Rh-based dinuclear building block (**1**) featuring a flexible configuration. Remarkably, multiple aromatic stacks were achieved by a guest-induced constitutional rearrangement, which provides vertical π-conjugations between NDI units and pyrene molecules. Furthermore, molecular BRs were constructed by precisely controlled noncovalent interactions. Our results thus show a simple approach to the creation and control of supramolecular architectures with intricate topology through stacking interactions, which has the potential to significantly impact strategies in the design of future molecular machines and functional nanodevices.

EXPERIMENTAL SECTION

General Methods. All reagents and solvents were purchased from commercial sources and used as supplied unless otherwise mentioned. The starting materials $[Cp^*MCl_2]_2$ (M = Rh, Ir),[21] [(*p*-cymene)-$RuCl_2]_2$,[22] and 2,7-dihydroxybenzo[*lmn*][3,8]phenanthroline-1,3,6,8-(2*H*,7*H*)-tetraone[23] (DHNDI) were prepared by a literature method. NMR spectra were recorded on Bruker AVANCE I 400 and VANCE-DMX 500 spectrometers. Spectra were recorded at room temperature and referenced to the residual protonated solvent for NMR spectra. Proton chemical shift (δH = 3.31 (CD_3OD), 1.94 (CD_3CN)) and δC values (49.00 (CD_3OD), 118.26 (CD_3CN)) are reported relative to the solvent residual peak. Coupling constants are expressed in hertz. Elemental analyses were performed on an Elementar Vario EL III analyzer. IR spectra of the solid samples (KBr tablets) in the range 400−4000 cm^{-1} were recorded on a Nicolet AVATAR-360IR spectrometer. ESI-MS spectra were recorded on a Micro TOF II mass spectrometer and a Waters Synapt G2 mass spectrometer using electrospray ionization.

Synthesis of 1. AgOTf (51 mg, 0.2 mmol) was added to a solution of $[Cp^*RhCl_2]_2$ (31 mg, 0.05 mmol) in CH_3OH (20 mL) at room temperature. The reaction mixture was stirred in the dark for 24 h and then filtered. DHNDI (15 mg, 0.05 mmol) and NaOH (4 mg, 0.1 mmol) were added to the filtrate. The mixture was stirred at room temperature for 24 h to give a dark red solution. The solvent was concentrated to about 3 mL. Upon the addition of diethyl ether, a dark solid was precipitated and collected. The product was recrystallized from a CH_3OH/diethyl ether mixture to afford a black solid.

Characterization data for **1** follow: 50 mg, yield 94%. ^1H NMR (400 MHz, CD_3OD, ppm): δ = 8.81 (s, 4H, NDI-H), 1.83 (s, 30H, Cp*-H). $^{13}C\{^1H\}$ NMR (101 MHz, CD_3OD, ppm): δ = 8.93 (Cp*), 95.50 (d, J = 10.0 Hz, Cp*), 121.78 (q, J_{CF} = 320.0 Hz, SO_3CF_3), 125.72, 127.70, 132.58, 164.91 (C═O), 165.20 (C═O). ^{19}F NMR (376 MHz, CD_3OD, ppm): δ = −80.1 (s, OTf^-). IR (KBr disk, cm^{-1}): ν = 1685, 1624, 1586, 1555, 1501, 1458, 1385, 1353, 1267, 1168, 1031, 1000, 983, 753, 638, 564, 519. Anal. Calcd for $C_{36}H_{34}F_6Rh_2N_2O_{12}S_2$ (M = 1070.59): C, 40.39; H, 3.20; N, 2.62. Found: C, 40.24; H, 3.23; N, 2.58. ESI-MS: m/z = 921.01 (calcd for $[M - OTf]^+$ 921.00).

General Synthesis of Complex 2−6. One of pyrazine (4.0 mg, 0.05 mmol)/4,4′-bipyridine (bpy) (7.8 mg, 0.05 mmol)/*trans*-1,2-bis(4-pyridyl)-ethylene (bpe) (9.1 mg, 0.05 mmol)/1,4-bis(4-pyridyl)-benzene (bpb) (11.7 mg, 0.05 mmol)/*N*,*N*′-bis(4-pyridylformamide)-1,4-benzene (bpfb) (16.0 mg, 0.05 mmol) was added to a solution of **1** (0.05 mmol) in methanol. The mixture was then stirred for 24 h. The solution was filtered through Celite and evaporated to dryness. The product was crystallized from CH_3OH/ether.

Characterization data for **2** follow: 53 mg, yield 92%. ^1H NMR (400 MHz, CD_3OD, ppm): δ = 8.93 (br, 4H, NDI-H), 8.76 (br, 8H, pyrazine-H), 8.60 (br, 4H, NDI-H), 1.80 (br, 60H, Cp*-H). ^{19}F NMR (376 MHz, CD_3OD, ppm): δ = −80.1 (s, OTf^-). IR (KBr disk, cm^{-1}): ν = 1703, 1628, 1556, 1500, 1469, 1419, 1377, 1350, 1261, 1224, 1157, 1032, 993, 935, 891, 748, 638, 519. Anal. Calcd for $C_{80}H_{76}F_{12}Rh_4N_8O_{24}S_4$ (M = 2301.36): C, 41.75; H, 3.33; N, 4.87. Found: C, 41.62; H, 3.25; N, 4.96. ESI-TOF-MS: m/z = 1045.05 (calcd for $[M + 4Na^+ - 4H^+ - 2OTf^-]^{2+}$ 1045.01).

Characterization data for **3** follow: 58 mg, yield 94%. ^1H NMR (400 MHz, CD_3OD, ppm): δ = 8.76 (d, 8H, bpy-H), 8.72 (br, 4H, NDI-H), 8.60 (br, 4H, NDI-H), 7.98 (br, 8H, bpy-H), 1.75 (s, 60H, Cp*-H). $^{13}C\{^1H\}$ NMR (101 MHz, CD_3OD, ppm): δ = 8.67 (Cp*), 96.88 (d, J = 8.5 Hz, Cp*), 121.76 (q, J_{CF} = 320.2 Hz, SO_3CF_3), 125.37, 125.67, 126.55, 128.48, 131.82, 132.83, 147.39, 153.13, 162.08 (C═O), 168.11 (C═O). IR (KBr disk, cm^{-1}): ν = 1699, 1678, 1608, 1547, 1500, 1454, 1411, 1377, 1354, 1269, 1160, 1032, 1001, 984, 820, 750, 640, 575, 519. Anal. Calcd for $C_{92}H_{84}F_{12}Rh_4N_8O_{24}S_4$ (M = 2453.55): C, 45.04; H, 3.45; N, 4.57. Found: C, 45.13; H, 3.52; N, 4.65. ESI-TOF-MS: m/z = 1077.15 (calcd for $[M - 2H - 2OTf^-]^{2+}$ 1077.07).

Characterization data for **4** follow: 58 mg, yield 92%. ^1H NMR (400 MHz, CD_3OD, ppm): δ = 8.70 (br, 8H, NDI-H), 8.61 (d, 8H, bpe-H), 7.72 (d, 8H, bpe-H), 7.48 (s, 4H, bpe-H), 1.74 (s, 60H, Cp*-H). ^1H NMR (400 MHz, CD_3CN, ppm): δ = 8.54 (br, 8H, NDI-H), 8.51 (d, 8H, bpe-H), 7.63 (d, 8H, bpe-H), 7.41 (s, 4H, bpe-H), 1.66 (s, 60H, Cp*-H). $^{13}C\{^1H\}$ NMR (101 MHz, CD_3CN, ppm): δ = 8.87 (Cp*), 95.96 (d, J = 9.0 Hz, Cp*), 122.09 (q, J_{CF} = 322.4 Hz, SO_3CF_3), 124.74, 124.90, 126.49, 128.34, 130.92, 132.32, 147.17, 152.13, 161.40 (C═O), 167.80 (C═O). IR (KBr disk, cm^{-1}): ν = 1701, 1610, 1551, 1501, 1458, 1430, 1379, 1352, 1262, 1224, 1159, 1031, 999, 983, 838, 751, 638, 556, 518. Anal. Calcd for $C_{96}H_{88}F_{12}Rh_4N_8O_{24}S_4$ (M = 2505.63): C, 46.02; H, 3.54; N, 4.47. Found: C, 46.10; H, 3.59; N, 4.42. ESI-TOF-MS: m/z = 1012.06 (calcd for $[M + 2Na^+ + 4H_2O - 4H^+ - 4OTf^-]^{2+}$ 1012.14); m/z = 1103.59 (calcd for $[M - 2OTf^- - 6H]^{2+}$ 1103.59).

Characterization for **5** follow: 59 mg, yield 90%. ^1H NMR (400 MHz, CD_3CN, ppm): δ = 8.58 (br, 8H, NDI-H), 8.57 (d, 8H, bpb-H), 7.80 (d, 8H, bpb-H), 7.80 (s, 8H, bpb-H), 1.69 (s, 60H, Cp*-H). $^{13}C\{^1H\}$ NMR (101 MHz, CD_3CN, ppm): δ = 8.90 (Cp*), 95.93 (d, J = 8.9 Hz, Cp*), 122.11 (q, J_{CF} = 322.2 Hz, SO_3CF_3), 124.72, 126.60, 129.00, 131.00, 132.35, 138.18, 150.29, 152.16, 161.31 (C═O), 167.88 (C═O). IR (KBr disk, cm^{-1}): ν = 1706, 1610, 1551, 1501, 1430, 1379, 1262, 1224, 1158, 1031, 999, 983, 817, 750, 638, 573, 518. Anal. Calcd for $C_{104}H_{92}F_{12}Rh_4N_8O_{24}S_4$ (M = 2605.74): C, 47.94; H, 3.56; N, 4.30. Found: C, 47.78; H, 3.62; N, 4.35. ESI-TOF-MS: m/z = 719.10 (calcd for $[M - 3OTf^- - 3H]^{3+}$ 719.09); m/z = 1153.09 (calcd for $[M - 2OTf^- - 2H]^{2+}$ 1153.10).

Characterization for **6(BRs)** follow: 66 mg, yield 95%. ^1H NMR (400 MHz, CD_3OD, ppm): δ = 9.31 (d, J = 7.6 Hz, 6H, bpfb-H), 9.08 (d, J = 5.6 Hz, 12H, bpfb-H and br, 6H, NDI-H), 8.84−8.82 (br, 18H, NDI-H and d, J = 7.6 Hz, 6H, bpfb-H), 8.50 (d, J = 7.6 Hz, 6H, bpfb-H), 8.29 (d, J = 5.6 Hz, 12H, NDI-H), 8.05 (d, J = 7.6 Hz, 6H, bpfb-

DOI: 10.1021/jacs.6b11968
J. Am. Chem. Soc. 2017, 139, 1653−1660

H), 7.22 (br, 12H, bpfb-NH), 5.83 (d, J = 8.8 Hz, 12H, bpfb-H), 5.38 (d, J = 8.8 Hz, 12H, bpfb-H), 1.90 (s, 90H, Cp*-H), 1.85 (s, 90H, Cp*-H). ^{1}H NMR (400 MHz, CD_3CN, ppm): δ = 9.11 (d, J = 7.6 Hz, 6H, bpfb-H), 9.06 (s, 6H, NDI-H), 8.94 (d, J = 6.4 Hz, 12H, bpfb-H), 8.77 (s, 8H, NDI-H), 8.69 (d, J = 7.6 Hz, 6H, bpfb-H), 8.57 (d, J = 6.0 Hz, 12H, NDI-H), 8.48 (d, J = 7.6 Hz, 6H, bpfb-H), 8.19 (d, J = 6.4 Hz, 12H, bpfb-H), 7.95 (d, J = 7.6 Hz, 6H, bpfb-H), 6.96 (br, 12H, bpfb-NH), 5.75 (d, J = 8.8 Hz, 12H, bpfb-H), 5.34 (d, J = 8.8 Hz, 12H, bpfb-H), 1.86 (s, 90H, Cp*-H), 1.78 (s, 90H, Cp*-H). $^{13}C\{^1H\}$ NMR (101 MHz, CD_3CN, ppm): δ = 8.79 (Cp*), 8.89 (Cp*), 96.10 (d, J = 6.8 Hz, Cp*), 96.39 (d, J = 6.4 Hz, Cp*), 119.00, 121.11, 121.93, 122.28 (q, J_{CF} = 322.1 Hz, SO_3CF_3), 124.34, 124.88, 125.18, 125.72, 125.84, 126.94, 127.54, 127.60, 130.84, 132.26, 132.67, 132.81, 134.33, 143.93, 145.04, 152.18, 152.54, 152.95, 160.70 (C═O), 160.75 (C═O), 161.38 (C═O), 164.02 (C═O), 167.56 (C═O), 168.01 (C═O). IR (KBr disk, cm^{-1}): ν = 1701, 1671, 1610, 1551, 1515, 1406, 1380, 1319, 1263, 1225, 1161, 1062, 1031, 999, 983, 840, 751, 681, 638, 560, 518. Anal. Calcd for $C_{324}H_{288}F_{36}Rh_{12}N_{36}O_{84}S_{12}$ (M = 8333.53): C, 46.70; H, 3.48; N, 6.05. Found: C, 46.81; H, 3.40; N, 6.12. ESI-TOF-MS: m/z = 1517.34 (calcd for $[M - 5OTf^- - 7H]^{5+}$ 1517.33); m/z = 1581.51 (calcd for $[M + Na^+ - 3OTf^- - 8H]^{5+}$ 1581.51); m/z = 1933.72 (calcd for $[M - 4OTf^- - 6H]^{4+}$ 1933.90).

Characterization details for **6(monomeric rectangle)** follow. ^{1}H NMR (400 MHz, CD_3OD, ppm): δ = 8.84 (d, J = 6.4 Hz, 8H, bpfb-H), 8.71 (br, 8H, NDI-H), 7.98 (d, J = 6.4 Hz, 8H, bpfb-H), 7.69 (br, 4H, bpfb-NH), 7.59 (s, 8H, bpfb-H), 1.78 (s, 60H, Cp*). ^{1}H NMR (400 MHz, DMF-d_7, ppm): δ = 10.73 (br, 4H, bpfb-NH), 9.00 (d, J = 6.0 Hz, 8H, bpfb-H), 8.72 (br, 8H, NDI-H), 8.10 (d, J = 6.4 Hz, 8H, bpfb-H), 7.75 (s, 8H, bpfb-H), 1.82 (s, 60H, Cp*).

Synthesis of Cp*Ir-Based Borromean Rings 6′. AgOTf (51 mg, 0.2 mmol) was added to a solution of $[Cp^*IrCl_2]_2$ (40 mg, 0.05 mmol) in CH_3OH (20 mL) at room temperature. The reaction mixture was stirred in the dark for 24 h and then filtered. DHNDI (15 mg, 0.05 mmol), NaOH (4 mg, 0.1 mmol), and bpfb (16 mg, 0.05 mmol) were added to the filtrate. The reaction mixture was turned to a dark red solution and stirred for 24 h. The solvent was concentrated to about 3 mL. Upon the addition of diethyl ether, a dark solid was precipitated and collected, and dried under vacuum. The product was recrystallized from CH_3OH/DMF/diethyl ether: 70 mg, yield 89%.

Characterization data for **6′** follow. ^{1}H NMR (400 MHz, CD_3OD, ppm): δ = 9.38 (d, J = 7.2 Hz, 6H, bpfb-H), 9.08 (d, J = 6.4 Hz, 12H, bpfb-H and br, 6H, NDI-H), 8.92 (d, J = 7.2 Hz, 6H, bpfb-H), 8.86 (d, J = 5.6 Hz, 18H, NDI-H), 8.56 (d, J = 7.2 Hz, 6H, bpfb-H), 8.36 (d, J = 6.4 Hz, 12H, NDI-H), 8.09 (d, J = 6.0 Hz, 6H, bpfb-H), 7.38 (br, 12H, bpfb-NH), 5.89 (d, J = 8.8 Hz, 12H, bpfb-H), 5.44 (d, J = 8.8 Hz, 12H, bpfb-H), 1.86 (s, 90H, Cp*-H), 1.81 (s, 90H, Cp*-H). $^{13}C\{^1H\}$ NMR (101 MHz, CD_3OD, ppm): δ = 8.80 (Cp*), 8.85 (Cp*), 88.04 (Cp*), 88.46 (Cp*), 118.73, 120.75, 122.38 (q, J_{CF} = 321.4 Hz, SO_3CF_3), 125.23, 125.59, 125.87, 126.28, 126.55, 126.97, 127.96, 127.60, 128.10, 128.74, 131.50, 133.06, 133.72, 133.86, 134.35, 144.34, 145.89, 153.26, 153.47, 160.98 (C═O), 161.27 (C═O), 161.67 (C═O), 163.82 (C═O), 168.86 (C═O), 169.46 (C═O). IR (KBr disk, cm^{-1}): ν = 1713, 1669, 1611, 1548, 1515, 1497, 1470, 1405, 1385, 1319, 1262, 1161, 1062, 1031, 980, 839, 750, 684, 639, 574, 518.

Synthesis of Aromatic Stack 3a. A mixture of pyrene (12 mg, 0.06 mmol) and **3** (19 mg, 0.01 mmol) in CH_3OH (20 mL) was stirred for 24 h. The solvent was concentrated to about 3 mL. Upon the addition of diethyl ether, a dark solid was precipitated and collected, and dried under vacuum. The product was crystallized from DMF/CH_3OH/diethyl ether: 24 mg, yield 94%.

Characterization data for **3a** follow. ^{1}H NMR (400 MHz, CD_3OD, ppm): δ = 8.89 (br, 16H, bpy-H), 8.36 (br, 16H, NDI-H), 8.23 (br, 16H, bpy-H), 7.01 (br, 2H, pyrene-H), 6.75 (br, 4H, pyrene-H), 6.00 (br, 4H, pyrene-H), 1.73 (s, 120H, Cp*-H). IR (KBr disk, cm^{-1}): ν = 1713, 1609, 1552, 1500, 1468, 1413, 1377, 1258, 1223, 1156, 1072, 1030, 988, 932, 889, 843, 817, 744, 710, 638, 555, 517. Anal. Calcd for $C_{200}H_{178}F_{24}Rh_8N_{16}O_{48}S_8$ (M = 5109.36): C, 47.01; H, 3.51; N, 4.39. Found: C, 47.13; H, 3.55; N, 4.36. ESI-TOF-MS: m/z = 1128.19 (calcd for $[M - 4OTf^- - 4H]^{4+}$ 1128.09); m/z = 1554.17 (calcd for $[M - 3OTf^- - 2H]^{3+}$ 1554.11).

Synthesis of (*p*-Cymene)Ru-Based Metallarectangle 4′. AgOTf (51 mg, 0.2 mmol) was added to a solution of $[(p\text{-cymene})RuCl_2]_2$ (31 mg, 0.05 mmol) in CH_3OH (20 mL) at room temperature. The reaction mixture was stirred in the dark for 24 h and then filtered. DHNDI (15 mg, 0.05 mmol), NaOH (4 mg, 0.1 mmol), and bpe (9 mg, 0.05 mmol) were added to the filtrate. The reaction mixture turned into a dark red solution in several minutes and was stirred for 24 h. The solvent was concentrated to about 3 mL. Upon the addition of diethyl ether, a dark solid was precipitated and collected, and dried under vacuum. The product was recrystallized from CH_3OH/DMF/diethyl ether: 56 mg, yield 90%.

Characterization for **4′** follow. ^{1}H NMR (400 MHz, CD_3OD, ppm): δ = 8.74 (br, NDI-H), 8.72 (br, NDI-H), 8.69−8.62 (m, NDI-H), 8.61−8.55 (m, 8H, bpe-H), 7.64−7.61 (m, 8H, bpe-H), 7.44−7.40 (m, 4H, bpe-H), 7.41 (s, 4H, bpe-H), 6.05−6.00 (m, 4H, cymene-H), 5.96−5.92 (m, 4H, cymene-H), 5.82−5.74 (m, 8H, cymene-H), 2.91−2.84 (m, 4H, cymene-H), 2.18 (br, 12H, cymene-H), 1.37−1.31 (m, 24H, cymene-H). IR (KBr disk, cm^{-1}): ν = 1706, 1611, 1585, 1548, 1500, 1471, 1431, 1392, 1355, 1271, 1225, 1162, 1059, 1030, 981, 882, 837, 751, 638, 574, 518. Anal. Calcd for $C_{96}H_{84}F_{12}Ru_4N_8O_{24}S_4$ (M = 2494.25): C, 46.23; H, 3.39; N, 4.49. Found: C, 46.28; H, 3.35; N, 4.52.

Synthesis of Aromatic Stack 4a/4a′. A mixture of pyrene (20 mg, 0.1 mmol) and **4** (25 mg, 0.01 mmol)/**4′** (25 mg, 0.01 mmol) in CH_3OH (20 mL) was stirred for 24 h. Dark colored crystalline deposits were formed. The product was washed with diethyl ether and dried under vacuum.

Characterization data for **4a** follow. ^{1}H NMR (400 MHz, CD_3OD, ppm): δ = 8.92−8.89 (d, J = 4.8 Hz, 8H, bpe-H and d, J = 6.0 Hz, 8H, bpe-H), 8.26−8.24 (d, J = 5.2 Hz, 8H, bpe-H and d, J = 5.6 Hz, 8H, bpe-H), 8.12 (br, 12H, NDI-H), 8.02−7.91 (d, J = 16.4 Hz, 4H, and d, J = 16.8 Hz, 4H, bpe-H), 7.64 (s, 4H, pyrene-H), 6.66 (br, 4H, pyrene-H), 6.29 (br, 8H, NDI-H and pyrene-H), 5.97 (t, J = 7.6 Hz, 2H, pyrene-H), 5.86 (br, 4H-pyrene), 4.89 (d, J = 7.6 Hz, 2H, pyrene-H), 4.48 (s, 4H, pyrene-H), 2.93 (s, 4H, pyrene-H), 2.01 (s, 60H, Cp*-H), 1.69 (s, 60H, Cp*-H). IR (KBr disk, cm^{-1}): ν = 1705, 1609, 1556, 1501, 1467, 1429, 1376, 1260, 1224, 1159, 1067, 1031, 989, 844, 745, 712, 639, 558, 518.

Characterization data for **4a′** follow. ^{1}H NMR (400 MHz, CD_3OD, ppm): δ = 8.90−8.86 (d, J = 8.0 Hz, 8H, bpe-H and d, J = 6.8 Hz, 8H, bpe-H), 8.22 (br, 12H, NDI-H), 8.17−8.14 (d, J = 6.0 Hz, 8H, bpe-H and d, J = 6.4 Hz, 8H, bpe-H), 7.97−7.85 (d, J = 16.4 Hz, 4H, and d, J = 16.4 Hz, 4H, bpe-H), 7.50 (s, 4H, pyrene-H), 6.53 (br, 4H, pyrene-H), 6.26 (d, J = 6.0 Hz, 8H, cymene-H), 6.25 (br, 4H, pyrene-H), 6.02 (d, J = 6.8 Hz, 8H, cymene-H), 6.00 (br, 4H, pyrene-H), 5.99 (br, 4H, NDI-H), 5.97 (d, J = 6.0 Hz, 4H, cymene-H), 5.91 (d, J = 6.0 Hz, 4H, cymene-H), 5.85 (t, J = 7.6 Hz, 2H, pyrene-H), 5.78 (d, J = 6.0 Hz, 4H, cymene-H), 5.76 (d, J = 6.4 Hz, 4H, cymene-H), 4.69 (d, J = 7.6 Hz, 4H, pyrene-H), 4.29 (s, 4H, pyrene-H), 3.20−3.13 (m, J = 6.8 Hz, 4H, cymene-H), 2.88 (s, 4H, pyrene-H), 2.88−2.81 (m, J = 6.8 Hz, 4H, cymene-H), 2.52 (s, 12H, cymene-H), 2.21 (s, 12H, cymene-H), 1.73−1.69 (d, J = 7.2 Hz, 24H, cymene-H and d, J = 6.8 Hz, 12H, cymene-H), 1.33−1.31 (d, J = 7.2 Hz, 12H, cymene-H and d, J = 6.8 Hz, 12H, cymene-H). IR (KBr disk, cm^{-1}): ν = 1714, 1609, 1582, 1549, 1498, 1466, 1433, 1405, 1380, 1348, 1261, 1224, 1158, 1060, 1030, 988, 933, 891, 844, 756, 743, 712, 638, 572, 517.

Conditions for Crystal Growing of 4a′. Initial attempts to obtain single crystals suitable for X-ray analysis were fruitless. This problem was overcome by a heterogeneous layer diffusion process, where a CH_3OH solution of **4a′** was placed at the bottom of a culture tube, followed by careful layering of a hexane solution of pyrene (excess). Bulk-like black crystals grew on the tube wall within a few days.

■ ASSOCIATED CONTENT

Supporting Information

The Supporting Information is available free of charge on the ACS Publications website at DOI: 10.1021/jacs.6b11968.

Spectroscopic data and computational details (PDF)

DOI: 10.1021/jacs.6b11968
J. Am. Chem. Soc. 2017, 139, 1653−1660

X-ray crystallographic file for **1**, **2**, **3**, **3a**, and **4** (CIF)
X-ray crystallographic file for **4a′** and **5** (CIF)
X-ray crystallographic file for **6** (CIF)

AUTHOR INFORMATION

Corresponding Author

*gxjin@fudan.edu.cn

ORCID

Guo-Xin Jin: 0000-0002-7149-5413

Notes

The authors declare no competing financial interest.

ACKNOWLEDGMENTS

This work was supported by the National Science Foundation of China (21531002, 21374019), the Program for Changjiang Scholars and Innovative Research Team in University (IRT-15R12), and the Shanghai Science Technology Committee (13JC1400600, 16ZD2270100).

REFERENCES

(1) (a) Gianneschi, N. C.; Masar, M. S.; Mirkin, C. A. *Acc. Chem. Res.* **2005**, *38*, 825−837. (b) Oliveri, C. G.; Ulmann, P. A.; Wiester, M. J.; Mirkin, C. A. *Acc. Chem. Res.* **2008**, *41*, 1618−1629. (c) Wiester, M. J.; Ulmann, P. A.; Mirkin, C. A. *Angew. Chem., Int. Ed.* **2011**, *50*, 114−137. (d) Fujita, M.; Tominaga, M.; Hori, A.; Therrien, B. *Acc. Chem. Res.* **2005**, *38*, 369−378. (e) Pluth, M. D.; Bergman, R. G.; Raymond, K. N. *Acc. Chem. Res.* **2009**, *42*, 1650−1659. (f) Han, Y.-F.; Jia, W.-G.; Yu, W.-B.; Jin, G.-X. *Chem. Soc. Rev.* **2009**, *38*, 3419−3434. (g) Yoshizawa, M.; Klosterman, J. K.; Fujita, M. *Angew. Chem., Int. Ed.* **2009**, *48*, 3418−3438.

(2) (a) De, S.; Mahata, K.; Schmittel, M. *Chem. Soc. Rev.* **2010**, *39*, 1555−1575. (b) Ariga, K.; Ito, H.; Hill, J. P.; Tsukube, H. *Chem. Soc. Rev.* **2012**, *41*, 5800−5835. (c) Ward, M. D.; Raithby, P. R. *Chem. Soc. Rev.* **2013**, *42*, 1619−1636. (d) Custelcean, R. *Chem. Soc. Rev.* **2014**, *43*, 1813−1824. (e) Schmidt, A.; Kühn, A. C. E.; Casini, A. *Coord. Chem. Rev.* **2014**, *275*, 19−36. (f) Han, M.; Engelhard, D. M.; Clever, G. H. *Chem. Soc. Rev.* **2014**, *43*, 1848−1860.

(3) (a) Northrop, B. H.; Zheng, Y.-R.; Chi, K.-W.; Stang, P. J. *Acc. Chem. Res.* **2009**, *42*, 1554−1563. (b) Chakrabarty, R.; Mukherjee, P. S.; Stang, P. J. *Chem. Rev.* **2011**, *111*, 6810−6918. (c) Cook, T. R.; Vajpayee, V.; Lee, M. H.; Stang, P. J.; Chi, K.-W. *Acc. Chem. Res.* **2013**, *46*, 2464−2474. (d) Cook, T. R.; Zheng, Y. R.; Stang, P. J. *Chem. Rev.* **2013**, *113*, 734−777. (e) Mukherjee, S.; Mukherjee, P. S. *Chem. Commun.* **2014**, *50*, 2239−2248. (f) Cook, T. R.; Stang, P. J. *Chem. Rev.* **2015**, *115*, 7001−7045. (g) Saha, M. L.; Yan, X.; Stang, P. J. *Acc. Chem. Res.* **2016**, *49*, 2527−2539.

(4) (a) Amouri, H.; Desmarets, C.; Moussa, J. *Chem. Rev.* **2012**, *112*, 2015−2041. (b) Smulders, M. M.; Riddell, I. A.; Browne, C.; Nitschke, J. R. *Chem. Soc. Rev.* **2013**, *42*, 1728−1754. (c) Han, Y.-F.; Jin, G.-X. *Acc. Chem. Res.* **2014**, *47*, 3571−3579. (d) Zarra, S.; Wood, D. M.; Roberts, D. A.; Nitschke, J. R. *Chem. Soc. Rev.* **2015**, *44*, 419−432. (e) Xu, L.; Wang, Y.-X.; Chen, L.-J.; Yang, H.-B. *Chem. Soc. Rev.* **2015**, *44*, 2148−2167.

(5) Mirtschin, S.; Slabon-Turski, A.; Scopelliti, R.; Velders, A. H.; Severin, K. *J. Am. Chem. Soc.* **2010**, *132*, 14004−14005.

(6) Boehr, D. D.; Nussinov, R.; Wright, P. E. *Nat. Chem. Biol.* **2009**, *5*, 789−796.

(7) (a) McConnell, A. J.; Wood, C. S.; Neelakandan, P. P.; Nitschke, J. R. *Chem. Rev.* **2015**, *115*, 7729−7793. (b) Wang, W.; Wang, Y.-X.; Yang, H.-B. *Chem. Soc. Rev.* **2016**, *45*, 2656−2693.

(8) (a) Lehn, J.-M. *Supramolecular Chemistry. Concepts and Perspectives*; Wiley-VCH: Weinheim, Germany, 1995. (b) Meyer, E. A.; Castellano, R. K.; Diederich, F. *Angew. Chem., Int. Ed.* **2003**, *42*, 1210−1250. (c) Salonen, L. M.; Ellermann, M.; Diederich, F. *Angew. Chem., Int. Ed.* **2011**, *50*, 4808−4842. (d) Li, S.; Huang, J.; Zhou, F.; Cook, T. R.; Yan, X.; Ye, Y.; Zhu, B.; Zheng, B.; Stang, P. J. *J. Am. Chem. Soc.* **2014**, *136*, 5908−5911. (e) Ye, Y.; Wang, S.-P.; Zhu, B.; Cook, T. R.; Wu, J.; Li, S.; Stang, P. J. *Org. Lett.* **2015**, *17*, 2804−2807.

(9) (a) Mahadevi, A. S.; Sastry, G. N. *Chem. Rev.* **2016**, *116*, 2775−2825. (b) Li, S.; Cooper, V. R.; Thonhauser, T.; Lundqvist, B. I.; Langreth, D. C. *J. Phys. Chem. B* **2009**, *113*, 11166−11172. (c) Müller-Dethlefs, K.; Hobza, P. *Chem. Rev.* **2000**, *100*, 143−168. (d) Burley, S.; Petsko, G. *Science* **1985**, *229*, 23−28.

(10) (a) Harmata, M. *Acc. Chem. Res.* **2004**, *37*, 862−873. (b) Yamauchi, Y.; Yoshizawa, M.; Fujita, M. *J. Am. Chem. Soc.* **2008**, *130*, 5832−5833. (c) Forgan, R. S.; Sauvage, J.-P.; Stoddart, J. F. *Chem. Rev.* **2011**, *111*, 5434−5464. (d) Beves, J. E.; Blight, B. A.; Campbell, C. J.; Leigh, D. A.; McBurney, R. T. *Angew. Chem., Int. Ed.* **2011**, *50*, 9260−9327. (e) Li, S.; Huang, J.; Cook, T. R.; Pollock, J. B.; Kim, H.; Chi, K.-W.; Stang, P. J. *J. Am. Chem. Soc.* **2013**, *135*, 2084−2087. (f) Yan, X.; Li, S.; Cook, T. R.; Ji, X.; Yao, Y.; Pollock, J. B.; Shi, Y.; Yu, G.; Li, J.; Huang, F.; Stang, P. J. *J. Am. Chem. Soc.* **2013**, *135*, 14036−14039. (g) Ayme, J.-F.; Beves, J. E.; Campbell, C. J.; Leigh, D. A. *Chem. Soc. Rev.* **2013**, *42*, 1700−1712. (h) Gil-Ramírez, G.; Leigh, D. A.; Stephens, A. J. *Angew. Chem., Int. Ed.* **2015**, *54*, 6110−6150.

(11) (a) Chichak, K. S.; Cantrill, S. J.; Pease, A. R.; Chiu, S.-H.; Cave, G. W. V.; Atwood, J. L.; Stoddart, J. F. *Science* **2004**, *304*, 1308−1312. (b) Cantrill, S. J.; Chichak, K. S.; Peters, A. J.; Stoddart, J. F. *Acc. Chem. Res.* **2005**, *38*, 1−9. (c) Meyer, C. D.; Forgan, R. S.; Chichak, K. S.; Peters, A. J.; Tangchaivang, N.; Cave, G. W. V.; Khan, S. I.; Cantrill, S. J.; Stoddart, J. F. *Chem. - Eur. J.* **2010**, *16*, 12570−12581. (d) Kim, T.; Singh, N.; Oh, J.; Kim, E.-H.; Jung, J.; Kim, H.; Chi, K.-W. *J. Am. Chem. Soc.* **2016**, *138*, 8368−8371.

(12) (a) Leigh, D. A.; Pritchard, R. G.; Stephens, A. J. *Nat. Chem.* **2014**, *6*, 978−982. (b) Marcos, V.; Stephens, A. J.; Jaramillo-Garcia, J.; Nussbaumer, A. L.; Woltering, S. L.; Valero, A.; Lemonnier, J. F.; Vitorica-Yrezabal, I. J.; Leigh, D. A. *Science* **2016**, *352*, 1555−1559.

(13) (a) Engelhard, D. M.; Freye, S.; Grohe, K.; John, M.; Clever, G. H. *Angew. Chem., Int. Ed.* **2012**, *51*, 4747−4750. (b) Zhang, G.; Gil-Ramírez, G.; Markevicius, A.; Browne, C.; Vitorica-Yrezabal, I. J.; Leigh, D. A. *J. Am. Chem. Soc.* **2015**, *137*, 10437−10442.

(14) (a) Pentecost, C. D.; Chichak, K. S.; Peters, A. J.; Cave, G. W. V.; Cantrill, S. J.; Stoddart, J. F. *Angew. Chem., Int. Ed.* **2007**, *46*, 218−222. (b) Schouwey, C.; Holstein, J. J.; Scopelliti, R.; Zhurov, K. O.; Nagornov, K. O.; Tsybin, Y. O.; Smart, O. S.; Bricogne, G.; Severin, K. *Angew. Chem., Int. Ed.* **2014**, *53*, 11261−11265. (c) Beves, J. E.; Danon, J. J.; Leigh, D. A.; Lemonnier, J.-F.; Vitorica-Yrezabal, I. J. *Angew. Chem., Int. Ed.* **2015**, *54*, 7555−7559. (d) Song, Y. H.; Singh, N.; Jung, J.; Kim, H.; Kim, E.-H.; Cheong, H.-K.; Kim, Y.; Chi, K.-W. *Angew. Chem., Int. Ed.* **2016**, *55*, 2007−2011.

(15) (a) Champin, B.; Mobian, P.; Sauvage, J.-P. *Chem. Soc. Rev.* **2007**, *36*, 358−366. (b) Kay, E. R.; Leigh, D. A.; Zerbetto, F. *Angew. Chem., Int. Ed.* **2007**, *46*, 72−191. (c) Balzani, V.; Credi, A.; Venturi, M. *Molecular Devices and Machines*; Wiley-VCH: Weinheim, 2008.

(16) Li, H.; Zhang, H.; Lammer, A. D.; Wang, M.; Li, X.; Lynch, V. M.; Sessler, J. L. *Nat. Chem.* **2015**, *7*, 1003−1008.

(17) (a) Cougnon, F. B. L.; Au-Yeung, H. Y.; Pantoş, D. G.; Sanders, J. K. M. *J. Am. Chem. Soc.* **2011**, *133*, 3198−3207. (b) Cougnon, F. B. L.; Ponnuswamy, N.; Jenkins, N. A.; Pantoş, D. G.; Sanders, J. K. M. *J. Am. Chem. Soc.* **2012**, *134*, 19129−19135. (c) Black, S. P.; Stefankiewicz, A. R.; Smulders, M. M. J.; Sattler, D.; Schalley, C. A.; Nitschke, J. R.; Sanders, J. K. M. *Angew. Chem., Int. Ed.* **2013**, *52*, 5749−5752. (d) Ponnuswamy, N.; Cougnon, F. B. L.; Pantoş, D. G.; Sanders, J. K. M. *J. Am. Chem. Soc.* **2014**, *136*, 8243−8251. (e) Ronson, T. K.; Roberts, D. A.; Black, S. P.; Nitschke, J. R. *J. Am. Chem. Soc.* **2015**, *137*, 14502−14512.

(18) In the formation of **4′**, $[(p\text{-cymene})RuCl_2]_2$ was employed instead of $[Cp^*RhCl_2]$.

(19) (a) Huang, S.-L.; Lin, Y.-J.; Hor, T. S. A.; Jin, G.-X. *J. Am. Chem. Soc.* **2013**, *135*, 8125−8128. (b) Huang, S.-L.; Lin, Y.-J.; Li, Z.-H.; Jin, G.-X. *Angew. Chem., Int. Ed.* **2014**, *53*, 11218−11222.

(20) Vögtle, F.; Dünnwald, T.; Schmidt, T. *Acc. Chem. Res.* **1996**, *29*, 451−460.

(21) White, C.; Yates, A.; Maitlis, P. M.; Heinekey, D. M. *Inorg. Synth.* **1992**, *29*, 228−234.

DOI: 10.1021/jacs.6b11968
J. Am. Chem. Soc. 2017, 139, 1653−1660

(22) Bennett, M. A.; Huang, T. N.; Matheson, T. W.; Smith, A. K.; Ittel, S.; Nickerson, W. *Inorg. Synth.* **1982**, *21*, 74−78.
(23) Kantchev, E. A. B.; Tan, H. S.; Norsten, T. B.; Sullivan, M. B. *Org. Lett.* **2011**, *13*, 5432−5435.

DOI: 10.1021/jacs.6b11968
J. Am. Chem. Soc. 2017, 139, 1653−1660